

Isolation and characterization of a novel chicken astrovirus in China

Lijuan Yin, Qi Zhou, Kaijie Mai, Jianfei Huang, Zhuanqiang Yan, Xiaona Wei, Hanqin Shen, Qunhui Li, Li Chen, and Qingfeng Zhou¹

Wen's Group Academy, Wen's Foodstuffs Group Co, Ltd, Xinxing, Guangdong, 527400, China

ABSTRACT Chicken astrovirus (CAstV) is associated with kidney disease and visceral gout, runting and stunting syndrome, and white chick hatchery disease, causing economic losses to the poultry industry worldwide. In this study, 55.6% of 36 clinical samples from Guangdong province in China were positive for CAstV, but negative for other common enteric viruses, including avian nephritis virus, infectious bronchitis virus, fowl adenovirus Group I, Newcastle disease virus, chicken parvovirus, reovirus, and rotavirus by PCRs and RT-PCRs. A CAstV strain, named GD202013, was isolated from Guangdong province in south China, and was identified by CAstV RT-PCR. A whole genome sequence analysis demonstrated that GD202013 shares 76.0 to 88.1% identity with 24

reference strains in GenBank. Phylogenetic analysis, based on whole genome and capsid protein, showed that GD202013 is more closely related to 2 US strains (GA2011/US/2011 and 4175/US/2011) belonging to subgroup Bii. Recombination analysis indicated that GD202013 is a recombinant strain formed by 3 strains: a major parent strain CkP5/US/2016, and 2 minor parent strains (GA2011/US/2011 and G059/PL/2014). In addition, the chicken embryo infection experiment demonstrated that GD202013 causes hatchability reduction, growth depression, and death of embryos. Macroscopic and microscopic lesions in the liver, kidney and small intestine were observed in the dead-in-shell embryos. This is the first report of the novel CAstV infection in China.

Key words: chicken astrovirus, isolation, complete genome, recombination analysis

2021 Poultry Science 100:101363

<https://doi.org/10.1016/j.psj.2021.101363>

INTRODUCTION

Chicken astrovirus (CAstV), belonging to the *Avastrovirus II* species in the genus *Avastrovirus* within the *Astroviridae* family, has recently emerged as an important pathogen in chicken flocks (Walker et al., 2019). CAstV infections have been reported in many regions around the world, such as Asia, Europe, America, and India (Pantin-Jackwood et al., 2008; Smyth et al., 2012; Smyth, 2017; Xue et al., 2017; Palomino-Tapia et al., 2020; Xue et al., 2020). Chicken astrovirus is a non-enveloped, small (28–30 nm in diameter), single-stranded and positive-sense RNA virus with a genome of approximately 7.5 kb in length, coding for three open reading frames (ORFs) (Smyth, 2017). The genome organization of CAstV is similar to other astroviruses, with an order of 5'-untranslated region (5'-UTR), open reading frame 1a (ORF1a, protease), open reading

frame 1b (ORF1b, RNA-dependent RNA polymerase), open reading frame 2 (ORF2, capsid protein) and 3'-untranslated region (3'-UTR) (Sajewicz-Krukowska and Domanska-Blicharz, 2016). The ORF2 gene of viral capsid protein, the most hypervariable regions of the whole genome, is responsible for the variation in antigenicity and pathogenicity, and used for CAstV genotyping (Smyth et al., 2012). Based on the hypervariability of capsid protein, CAstV has been divided into 2 groups: Group A (3 subgroups: Ai, Aii, and Aiii) and Group B (4 subgroups: Bi, Bii, Biii, and Biv) (Smyth, 2017).

CAstV has been related to many diseases including enteric diseases, kidney diseases, visceral gout, and hatching problems in different countries of the world (Smyth, 2017). For example, CAstV has been associated with runting stunting syndrome (RSS), characterized by enteric diseases and growth problems. The disease was first described by Olsen, 1977 and Kouwenhoven et al. (1978), in chicken flocks with uneven growth. In addition, CAstV is also well-known for its association with kidney disease and visceral gout, characterized by high mortality in young broilers (up to 40%) in India in 2012 (Bulbule et al., 2013). Furthermore, CAstV has become associated with chick hatchery

© 2021 The Authors. Published by Elsevier Inc. on behalf of Poultry Science Association Inc. This is an open access article under the CC BY-NC-ND license (<http://creativecommons.org/licenses/by-nc-nd/4.0/>).

Received April 2, 2021.

Accepted June 22, 2021.

¹Corresponding author: zhqf1012@163.com

disease or “white chick” syndrome (**WCS**), characterized by reduction in hatchability (up to 68%) in several countries, including Canada, Ireland, Finland, Norway, Brazil, Poland, America, and the United Kingdom (Smyth et al., 2013; Nunez et al., 2016; Sajewicz-Krukowska et al., 2016; Palomino-Tapia et al., 2020).

In the present study, we isolated a novel chicken astrovirus strain from Guangdong province in China, and sequenced the complete genome of the new isolate. Sequence alignment, phylogenetic analysis, and recombination analysis were performed to compare GD202013 with other reference strains. The pathogenicity of this isolate to specific pathogen free (**SPF**) chicken embryos was investigated by hatchability and histology. This may provide valuable information about the evolution and pathogenicity of chicken astrovirus in the field.

MATERIALS AND METHODS

Clinical Samples, Macroscopic Lesions, and CAstV Detection by RT-PCR

In 2020, 36 clinical samples, such as small intestines and kidneys were collected from 6 different 1-day-old chicken flocks in Guangdong province. All of the selected flocks had growth problems and uneven size, and showed enteritis and kidney lesions (Supplementary Table S1). All tissue samples were homogenized in phosphate-buffered saline (**PBS**) and centrifuged at $6,000 \times g$ for 5 min after three freeze-thaw cycles, and the supernatant was used for virus isolation and viral DNA/RNA extraction by using a HiPure Viral RNA/DNA Kit (Magen, Guangzhou, China), according to manufacturer’s instructions. The presence of CAstV in tissue samples was confirmed with reverse transcription-polymerase chain reaction (**RT-PCR**) and sequencing analysis by GENEWIZ (Guangzhou, China). RT-PCR was performed using the primer pairs CAstV-F: 5’-KCA TGG CTY CAC CGY AAD CA-3’ and CAstV-R: 5’-CGG TCC ATC CCT CTA CCA GAT TT-3’ to amplify an approximately 510 bp product from the ORF1b gene, as previously described by Smyth et al. (2009). To detect potential viruses, including avian nephritis virus (**ANV**), chicken parvovirus (**ChPV**), avian reovirus, avian rotavirus, fowl adenovirus Group I (**FAdV-I**), Newcastle disease virus (**NDV**), and infectious bronchitis virus (**IBV**), each of these samples was examined for all 7 viruses by polymerase chain reaction (**PCR**) or RT-PCR using primers and methods as previously described (Nunez et al., 2015; Zhao et al., 2020).

Virus Isolation and Purification

Virus isolation and plaque purification were performed using leghorn male hepatoma (**LMH**) cells (ATCC #CRL-2117) as previously described with some modifications (Baxendale and Mebatsion, 2004; Zhao et al., 2020). For virus isolation, LMH cells were cultured in 6-well plates, and maintained in Dulbecco’s

Modified Eagle’s Medium (**DMEM**) medium (Hyclone, Logan, UT) supplemented with streptomycin (100 U/mL), penicillin (100 U/mL), and 10% fetal bovine serum (**FBS**) (BOVOGEN, Australia). The CAstV positive supernatant of tissue samples was filtered through a 0.22- μm syringe filter (Millipore, Cork, Ireland) and inoculated onto LMH cells. After 1 h absorption, the supernatant was replaced with DMEM medium supplemented with 2% FBS (henceforth referred to as maintenance medium). After 3 days of incubation at 37°C in 5% CO₂, the supernatant and cells were harvested by 3 freeze-thaw cycles for the next round of virus propagation, plaque purification, and quantification real-time PCR (**qPCR**) detection (Smyth et al., 2010).

For virus plaque purification, LMH cells at 90% confluence in 6-well plates were infected with the viral inocula prepared at different serial dilutions of virus suspension. After 1 h incubation, the supernatant was discarded, and replaced with 2 mL maintenance medium containing 1% Agarose LM GQT (TaKaRa, Dalian). After 3 to 5 days of incubation, the plates were stained with 2 mL maintenance medium containing 0.01% Neutral red solution (Sigma, St. Louis, MO). The plaques were picked and propagated in 12-well plates until CPE was evident. The selected plaques of CAstV were used for viral propagation. The CAstV isolate, designated as GD202013, was obtained by the fifth passage in LMH cells and used for subsequent experiments. The tissue culture infective doses (**TCID₅₀**) assay was performed as previously described by Kang et al. (2018).

Immunofluorescence Assay

Immunofluorescence assay (**IFA**) was performed to observe CAstV-infected LMH cells as described previously with minor modifications (Kang et al., 2018). Briefly, LMH cells in 12-well plates were infected with CAstV at a multiplicity of infection (**MOI**) of 0.5. After 72 h, the cells were fixed with 4% paraformaldehyde for 30 min, and then permeabilized with 0.5% Triton X-100 for 30 min at room temperature. The cells were blocked with 2% bovine serum albumin (**BSA**) for 1 h at 37°C, and then incubated for 16 h at 4°C with CAstV specific mouse antisera (Wen’s Foodstuffs Group Co., Ltd, China) (1:200), followed by fluorescein isothiocyanate (**FITC**)-labeled goat anti-mouse IgG secondary antibody (Beyotime, Shanghai, China) (1:500) for 1 h at 37°C. Cell nuclei were stained with 4’-6’-diamidino-2-phenylindole (**DAPI**) (Beyotime, Shanghai, China) for 10 min. Then, the stained cells were observed with a fluorescence microscope (IX73, Olympus, Japan).

Next-Generation Sequencing

The genomic sequence of the GD202013 strain was sequenced by nanopore sequencing technology (Oxford Nanopore, UK) as previously described with some modifications (Li et al., 2020; Palomino-Tapia et al., 2020). Briefly, total RNA was extracted from infected LMH

culture supernatant using TRIzol Reagent (Invitrogen, Carlsbad, CA), and treated with RNase-free DNase I (Qiagen, Hilden, Germany) to remove any DNA contamination following the manufacturer's protocols. The total RNA was used as the template for cDNA synthesis using The Maxima H Minus Double-Stranded cDNA Synthesis Kit (Thermo Scientific, Vilnius, Lithuania), and the residual RNA was removed from the double-stranded cDNA preparation, according to the manufacturer's instructions. Then the double-stranded cDNA was purified using a 1:1 ratio of AMPure XP beads (Beckman, Brea, CA), and quantified using a Qubit high-sensitivity double-stranded DNA (**dsDNA**) kit (Thermo Fisher, Eugene, OR), both according to the manufacturer's protocols. Nanopore libraries were generated using 200 ng of cDNA per sample as input to the SQK-LSK109 kit, and barcoded individually using the EXP-NBD104 Native barcodes (Oxford Nanopore Technologies, UK). Libraries were loaded to a MinION Mk1B device (Oxford Nanopore Technologies, UK) for real-time single-molecule sequencing. All sample reads were mapped to the CAstV isolate CkP5 (GenBank number: KX397576), under the App Map function of CLC Genomics Workbench v 20.0.2 (Qiagen, Germany) using default settings as previously described (Palomino-Tapia et al., 2020). To validate the results of next-generation sequencing, PCR amplification and Sanger sequencing were done as described previously (Zhao et al., 2020).

Phylogenetic Analysis and Recombination Analysis

Comparison and analysis of the genome sequences, ORF1a, ORF1b, and ORF2 of the strain and the reference CAstV strains were conducted using the DNASTar software Lasergene 7.0. Sequence alignment analyses of genomes and predicted protein were performed using the Clustal W method, and phylogenetic trees were conducted by the neighbor-joining method in the MEGA 7.0 software. The bootstrap values were determined from 1,000 replicates (Zhao et al., 2020). To predict the possible recombination events in CAstV strain GD202013, the aligned sequences were analyzed using recombination detection program (**RDP**) software version 5.5 with the recombination detection methods (RDP, GENECONV, BootScan, MaxChi, Chimaera, SiScan and 3Seq) (Martin et al., 2015). Recombination events were detected by at least 6 of these methods. The potential recombination events and breakpoints were further verified by SimPlot version 3.5.1 (Lole et al., 1999), using the following parameters: window size = 200 bp; step size = 20 bp; GapStrip = On; Kimura 2-parameter substitution model; T/t = 2.

Pathogenicity Analysis

The experimental infection with the CAstV strain in chicken embryos was performed as previously described

with minor modifications (Zhao et al., 2020). Briefly, forty 8-day-old SPF chicken embryos (Guangdong Wens Dahuanong Biotechnology Co., Ltd., Guangdong, China) were divided into 2 groups (n = 20 chicken embryos/group). The infected group was inoculated with 0.2 mL of maintenance medium containing 10^4 TCID₅₀ of the CAstV GD202013 strain using the yolk-sac route. The negative control group was inoculated (0.2 mL/egg) with DMEM medium via the yolk-sac route. All chicken embryos were incubated at 37°C and 55% relative humidity with rotation up to the 18th day of embryonic development. During this period, the eggs were monitored daily for embryonic viability. Dead embryos from the infected group were necropsied. At necropsy, the fresh samples (heart, liver, spleen, lung, kidney, bursa of fabricius, pancreas, small intestine, proventriculus, gizzard, and brain) were collected. One part of the samples was used for virus distribution analysis by qPCR, whereas the other part of the samples was formalin-fixed for histopathology analysis. All animal experiments were performed strictly in accordance with the "Guidelines for Experimental Animals" of the Ministry of Science and Technology (Beijing, China).

Quantification Real-Time PCR Analysis

Various tissue samples were tested by a CAstV ORF1b gene-based real-time PCR as previously described with minor modifications (Smyth et al., 2010). And the chicken house-keeping gene, glyceraldehyde-3-phosphate dehydrogenase (**GADPH**), was applied as an internal control to normalize the calculation of viral genome loads as previously described (Li et al., 2007, 2013). Specific primers for the conserved regions of the CAstV ORF1b gene (forward primer: 5'-GCT GCT GCT GAA GAT ATA CAG-3'; reverse primer: 5'-CAT CCC TCT ACC AGA TTT TCT GAA A-3'), and specific primers for the chicken GADPH gene (forward primer: 5'-TGC CAT CAC AGC CAC ACA GAA G-3'; reverse primer: 5'-ACT TTC CCC ACA GCC TTA GCA G-3') were synthesized by GENEWIZ (Guangzhou, China). The analysis of real-time PCR was carried out with the Applied Biosystem 7500 Fast Real Time PCR System (Thermo Fisher, Marsiling, Singapore). The quantification real-time PCR was conducted using TB Green Premix Ex Taq II (Tli RNaseH Plus, Takara, China), following the manufacturer's instructions. The amplification conditions were as follows: 95°C for 30 s, and 40 cycles of 95°C for 3 s, 60°C for 30 s, and 1 cycle of 95°C for 15 s, 60°C for 1 min, and 95°C for 15 s. The final step was to obtain a melt curve for the PCR products to verify the specificity of the amplification. The RNAs of CAstV and GADPH were simultaneously amplified in triplicate on the same plate, and the GADPH gene was utilized as the reference gene. Therefore, we obtained 3 threshold cycle (**CT**) values for both CAstV and GADPH for each sample. Average of these CT values (CT_{CAstV}) and (CT_{GADPH}) were used to determine the

relative viral load of CAstV using the $2^{-\Delta\Delta CT}$ method described previously (Li et al., 2007).

Histopathology

For histopathological analysis, fresh tissue samples (heart, liver, spleen, lung, kidney, bursa of fabricius, pancreas, small intestine, proventriculus, gizzard, and brain) from the infected and control groups were collected separately, and fixed in 10% formalin solution for 3 d at room temperature. Those fixed samples were embedded in paraffin, cut into 4- μ m-thick sections, and mounted onto glass slides. Then, the sections were deparaffinized, rehydrated, and stained with hematoxylin and eosin (HE), the slides were examined and analyzed under conventional light microscopy.

Statistical Analyses

The experiments were performed at least 3 times independently with similar results. Data are shown as the mean \pm standard deviations (SD). The significance of the variability between the trials was analyzed using GraphPad Prism 6 software. Differences between samples were assessed by the Student's *t* test, and *P* values less than 0.05 ($P < 0.05$) were considered statistically significant.

RESULTS

Clinical History, Samples and Macroscopic Lesions, and Histopathology

In 2020, 36 clinical tissue samples of 1-day-old broiler chickens, including small intestines and kidneys, were collected from 6 different chicken flocks in Guangdong province. All of the selected flocks had growth problems and uneven size. By gross observation, those chickens exhibited enteritis (Supplementary Figure S1A) and swollen kidney (Supplementary Figure S1B). Histopathological analysis showed that necrosis and abscission are observed in epithelial cells of the small intestine (Supplementary Figure S1C), and dilated tubules filled with red blood cells, inflammatory cell infiltration, and necrosis of renal tubular epithelial cells are observed in the kidney (Supplementary Figure S1D).

Detection of CAstV Through RT-PCR Examination-Clinical Samples

In this study, 36 clinical samples were detected for CAstV, ANV, IBV, ChPV, FAdV-I, avian rotavirus, avian reovirus, and NDV by PCR or RT-PCR as previously described. Among them, 20 of the 36 (55.6%) clinical samples were positive for CAstV only using RT-PCR (Supplementary Figure S2) and confirmed by Sang sequencing.

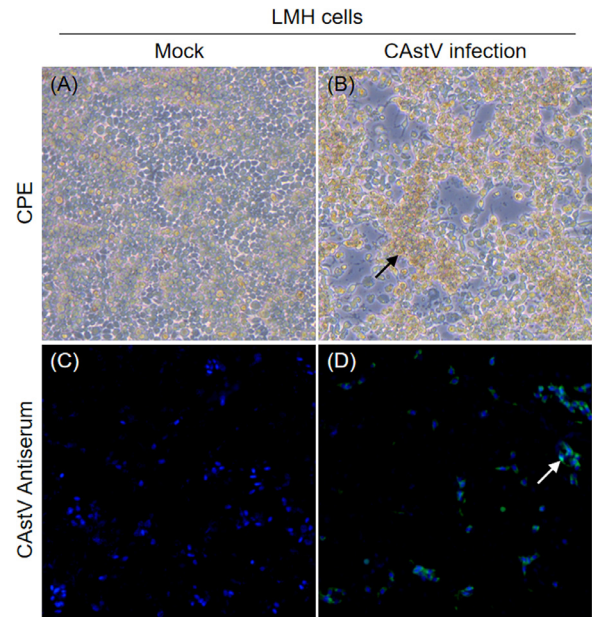


Figure 1. Isolation and identification of CAstV GD202013 in LMH cells. (A) Mock-infected LMH cell culture showing normal cells. (B) CAstV-infected LMH cells at 72 h postinfection showing detached small and round cells (indicated by arrow). (C, D) LMH cells were fixed and stained with CAstV specific mouse antisera and FITC-labeled goat anti-mouse secondary antibody at 72 h postinfection (green) (indicated by arrow), nuclei were stained with DAPI (blue). Magnification = 20 \times . Abbreviations: CAstV, chicken astrovirus; DAPI, 4',6'-diamidino-2-phenylindole; FITC, fluorescein isothiocyanate; LMH, leghorn male hepatoma.

Virus Isolation in LMH Cell Line

Those tissue samples that were only positive for CAstV were used to isolate CAstV using LMH cells. A CAstV strain was successfully isolated from one small intestine sample collected from chicken flock C with growth problem and diarrhea, namely GD202013. The cytopathic effect (CPE) of CAstV GD202013 in LMH cells was characterized by detached small and round cells at 72 h postinfection (Figure 1B), as compared with the control (Figure 1A), which is similar to the CPE described by Kang et al. (2018) and Zhao et al. (2020). After the fifth passage, the viral titer reached $10^{6.33}$ TCID₅₀/mL, showing that the GD202013 strain was highly replicative in LMH cells.

Immunofluorescence of Virus Propagation in LMH Cell Line

Virus propagation in LMH cells was demonstrated by IFA. LMH cells were infected with CAstV isolate GD202013 (passage five). At 72 h postinfection, the cells were fixed and then incubated with CAstV-specific mouse antisera at a 1:200 dilution, followed by FITC-conjugated goat anti-mouse IgG antibody at a 1:500 dilution, and nuclei were counterstained with DAPI at a 1:500 dilution. Finally, images were obtained using a fluorescence microscope. As shown in Figures 1C and 1D, blue fluorescence was observed in all LMH cells. However, green fluorescence was only observed in the

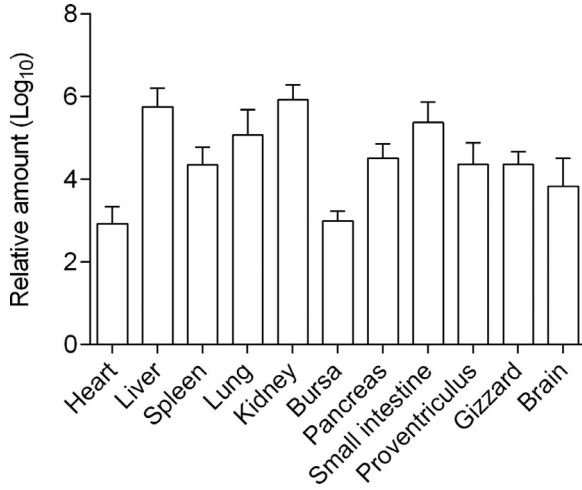


Figure 2. Virus distribution in various samples of CAstV-infected chicken embryos (n = 5 embryos). Abbreviation: CAstV, Chicken astrovirus.

CAstV-infected cells (Figure 1D), as compared to the control (Figure 1C), indicating that the GD202013 strain propagated in LMH cells.

Real Time RT-PCR for CAstV Quantification in the Cells and the Embryos

To confirm CAstV replication in LMH cells, viral RNA was extracted from the inoculated cells at 72 h postinfection and tested by specific real-time PCR. The result showed that the viral load continues to increase in LMH cells following 5 passages (Supplementary Figure S3). This cell culture-passaged sample was positive for

CAstV but negative for other common enteric viruses. Moreover, the viral RNA could be detected in all the samples of the infected dead-in-shell embryos. As shown in Figure 2, the general trend of tissue tropism for the samples according to the relative viral load of CAstV (from high to low) were as follows: kidney (average $10^{5.92}$), liver (average $10^{5.75}$), small intestine (average $10^{5.37}$), lung (average $10^{5.07}$), pancreas (average $10^{4.51}$), proventriculus (average $10^{4.37}$), gizzard (average $10^{4.36}$), spleen (average $10^{4.34}$), brain (average $10^{3.83}$), bursa of fabricius (average $10^{2.99}$), and heart (average $10^{2.92}$).

Genome Sequence Analysis

The whole genome sequence of GD202013 strain was determined by next-generation sequencing, and the sequence was verified by PCR amplification and Sanger sequencing as described previously. The complete sequence was deposited to the GenBank with accession number MW846319. The genome of GD202013 strain was 7,520 nucleotide (nt) in length, including 5'-UTR (21 nt), ORF1a (3,420 nt), ORF1b (1,560 nt), ORF2 (2,232 nt), and 3'-UTR (282 nt) sequences. As shown in Table 1, the sequence comparison analysis revealed that the nucleotide identity of the complete genome between GD202013 and 24 CAstV reference strains ranges from 76.0 to 88.1%. GD202013 had the highest resemblance to GA2011/US/2011 (subgroup Bii) with 88.1% identity and was least similar to G059/PL/2014 (subgroup Aiii) with 76.0% identity. The amino acid (aa) sequences of ORF1a and ORF1b of GD202013 strain shared the identities of 85.3 to 96.6% with the other CAstVs. In

Table 1. Comparison of the nucleotide and amino acid identities of the sequences of CAstV GD202013 strain with other representative CAstV strains.

Virus	Genotype	GenBank number	Sequence identity (%)			
			Genome (nt)	ORF1a (aa)	ORF1b (aa)	ORF2 (aa)
G059/PL/2014	Aiii	KT886453	76.0	93.5	96.3	40.3
HBLP717/1/CN/2018	Bi	MN725025	76.7	87.5	85.6	84.7
GDYHTJ718/6/CN/2018	Bi	MN725026	76.9	87.2	85.4	84.8
CZ1801/CN/2018	Bi	MN807051	76.7	87.2	85.8	84.9
NJ1701/CN/2017	Bi	MK746105	76.7	87.1	85.8	84.9
4175/US/2011	Bii	JF832365	87.3	95.4	85.3	90.7
GA2011/US/2011	Bii	JF414802	88.1	95.5	96.0	94.8
ANAND/IN/2016	Biii	KY038163	84.4	94.8	95.2	85.0
CC_CkAstV/US/2014	Biv	KX397575	86.0	96.5	95.4	86.0
CkP5/US/2016	Biv	KX397576	86.1	96.6	95.4	86.2
14/1235a/AB/2014	Biv	MT789774	85.9	95.2	95.4	86.2
14/1235b/AB/2014	Biv	MT789775	85.8	95.1	95.6	86.2
14/1235c/AB/2014	Biv	MT789776	85.8	95.2	95.4	86.2
14/1235d/AB/2014	Biv	MT789777	85.8	95.2	95.4	86.2
15/1262a/AB/2015	Biv	MT789778	85.8	95.4	95.4	85.9
15/1262b/AB/2015	Biv	MT789779	85.8	95.4	95.2	85.9
15/1262c/AB/2015	Biv	MT789780	85.8	95.4	95.4	85.9
15/1262d/AB/2015	Biv	MT789781	85.8	95.4	95.2	86.0
17/0773a/AB/2017	Biv	MT789782	85.2	95.1	95.2	85.9
17/0773b/AB/2017	Biv	MT789783	85.2	95.3	95.0	85.9
17/0823/AB/2017	Biv	MT789784	85.2	95.3	95.2	85.9
18/0942/SK/2018	Biv	MT789785	85.3	95.8	94.8	86.0
19/0935/SK/2019	Biv	MT789786	85.0	95.0	94.6	85.6
19/0981/SK/2019	Biv	MT789787	85.1	95.7	95.4	85.9

Abbreviation: CAstV, chicken astrovirus.

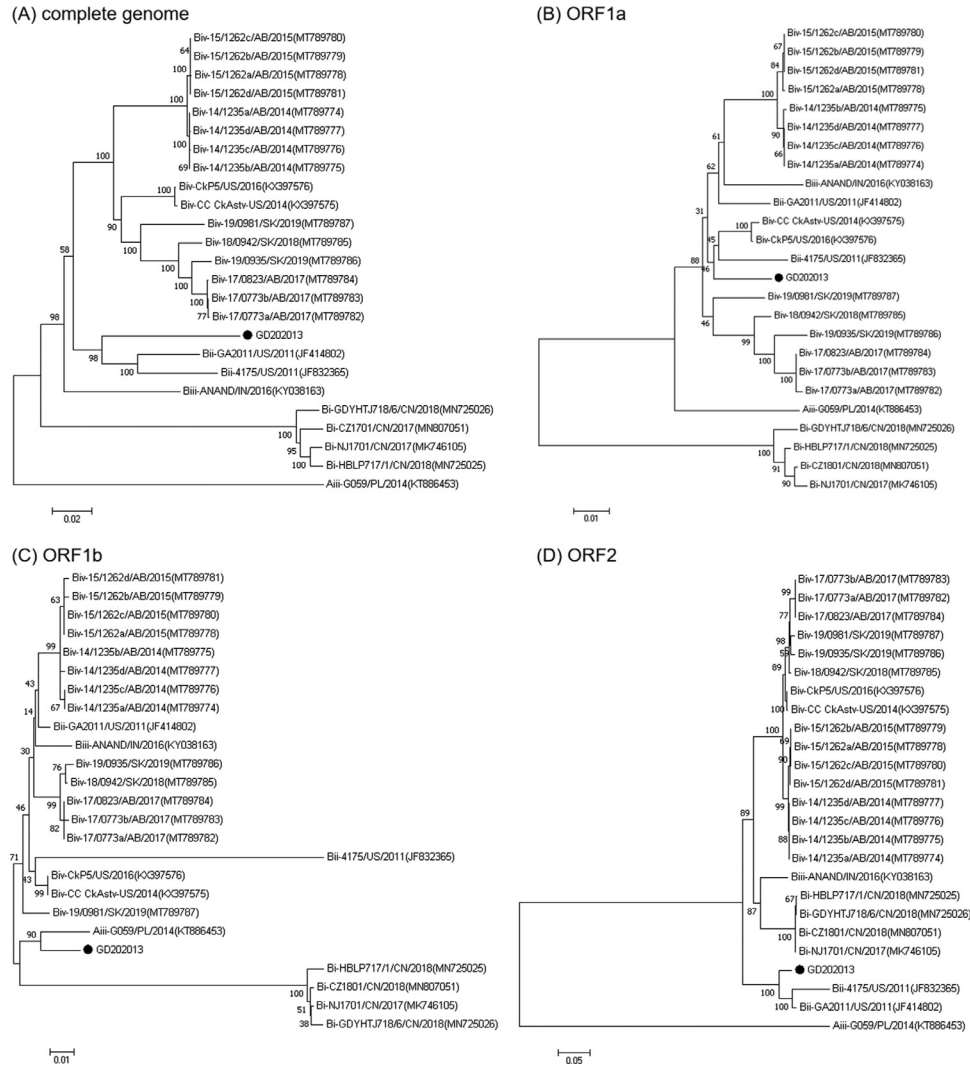


Figure 3. Phylogenetic analysis of CAstV strain GD202013. Phylogenetic trees based on the nucleotide sequences of complete genome (A), amino acid sequences of ORF1a (B), amino acid sequences of ORF1b (C), and amino acid sequences of ORF2 (D) were constructed using the neighbor-joining method in MEGA 7 (1,000 bootstrap replicate). The number in parenthesis indicates the GenBank accession number for each CAstV sequence. The new isolate is labeled with a black circle. Abbreviation: CAstV, chicken astrovirus.

addition, the amino acid sequence of ORF2 of GD202013 strain showed a high similarity (94.8%) with the GA2011/US/2011 strain and a low similarity (40.3%) with the G059/PL/2014 strain.

Phylogenetic Analysis and Determination of Recombination Events

To assess the genetic relatedness between GD202013 and the reference CAstV strains, phylogenetic trees were constructed for the nucleotide sequences of the complete genome and specific proteins of GD202013 and the 24 reference strains. As shown in Figure 3, phylogenetic analysis, based on whole genome and capsid (ORF2) protein, showed that GD202013 is more closely related to 2 US strains (GA2011/US/2011 and 4175/US/2011) belonging to the subgroup Bii. Nevertheless, the phylogenetic tree based on the ORF1b protein

showed that GD202013 strain is closely related to the G059/PL/2014 (subgroup Aiii) (Figure 3C).

In order to detect possible recombination events within the new isolate GD202013, recombination analysis was carried out using RDP and SimPlot software. The RDP analysis indicated that GD202013 is possibly a recombinant strain formed by three strains: a major parent (P1) strain CkP5/US/2016 and 2 minor parent (P2) strains GA2011/US/2011 and G059/PL/2014 (Table 2). It showed that the recombination breakpoints of GD202013 are mainly located at the 3,516 to 4,980 nt, and 5,558 to 7,038 nt (Table 2).

To confirm the results of the RDP analysis, genomic sequences analysis of GD202013, CkP5/US/2016, GA2011/US/2011 and G059/PL/2014 was carried out using the Simplot software. As shown in Figure 3, the recombination signals and the breakpoints of GD202013 were mainly located at the 4241-4881 nt (the region encoding ORF1b), and 5581-7161 nt (the region

Table 2. Details on recombination events detected by at least six methods on alignment of CAstV complete sequences.

Recombinant (R), major parent (P1) and minor parent (P2)	No. of recombination methods	<i>P</i> -value ranges	Position of breaking points
(R)-GD202013 P1-Biv-CkP5/US/2016 P2-Bii-GA2011/US/2011	7	1.974×10^{-17} - 1.081×10^{-34}	ORF2 Start: 5558 nt End: 7038 nt
(R)-GD202013 P1-Biv-CkP5/US/2016 P2-Aiii-G059/PL/2014	6	4.361×10^{-6} - 7.947×10^{-21} *	ORF1b Start: 3516 nt End: 4980 nt

*Recombination signal may be attributable to a process other than recombination.

encoding ORF2) (Figure 4A), which is similar to the RDP results (Table 2). In addition, phylogenetic trees of each recombinant region were constructed and analyzed, demonstrating that there is an alternation in the recombinant region of GD202013, which further confirms the recombination event (Figure 4B).

Pathogenicity of CAstV for Embryonated Eggs

The pathogenicity of CAstV strain GD202013 from passage 5 was demonstrated in the chicken embryos. The level of hatching rate in the control

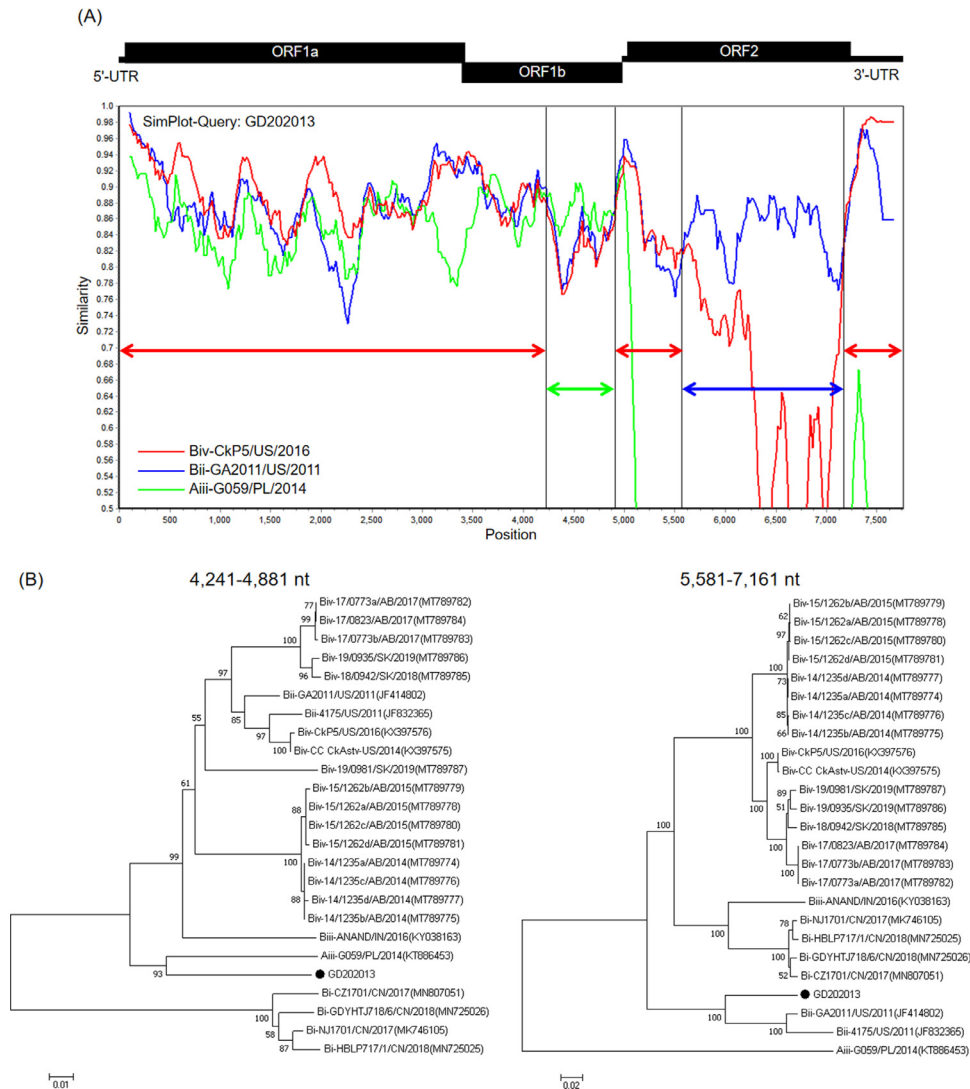


Figure 4. Recombination analysis of the complete genome of CAstV strain GD202013. SimPlot analysis was performed with GD202013 as the query sequence, and CkP5/US/2016 (red), GA2011/US/2011 (blue) and G059/PL/2014 (green) as putative parental strains. (A) The dummy lines show the deduced breakpoints at the genome positions 4,241 nt, 4,881 nt and 7,161 nt. Bars at the top demonstrate the relative positions of the genome of CAstV. The recombination region corresponding to the genome includes the ORF1b and ORF2 gene. (B) Phylogenetic trees of the genome regions 4,241 to 4,881 nt, and 5,581 nt to 7,161 nt among GD202013 and other 24 reference strains. Phylogenetic trees were constructed using the neighbor-joining method (bootstrapping for 1,000 replicates). Abbreviation: CAstV, chicken astrovirus.

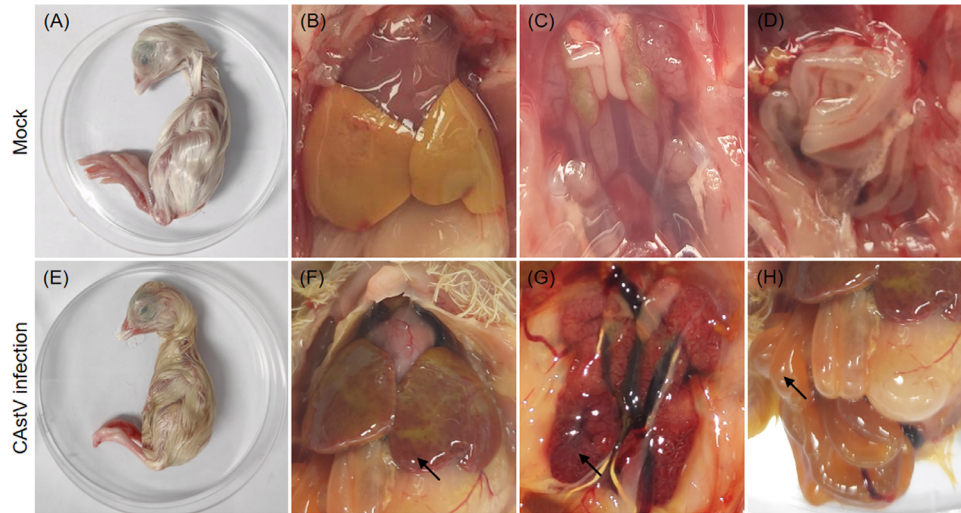


Figure 5. Infection experiments with CAstV GD202013 in chicken embryos. (A–D) Macroscopic picture of an 18-day-old control chicken embryo. (E–H) Macroscopic picture of an 18-day-old CAstV-infected chicken embryo. Dead-in-shell embryo showed growth depression, enlarged liver with numerous pinpoint hemorrhages, swollen and congested kidney, as well as gas-filled and liquid-filled intestine (indicated by arrows). Abbreviation: CAstV, chicken astrovirus.

group was 100%, and the chicken embryos did not show any necrotic lesions (Figures 5A–5D). However, all chickens in the infected group showed growth depression and stunted embryos (Figure 5E), with 0% hatching rate. And the major post-mortem findings of the dead-in-shell embryos were enlarged liver with numerous pinpoint hemorrhages on the surface (Figure 5F), swollen and congested kidney (Figure 5G), as well as intestines filled with yellow liquid content with the presence of bubbles of gas

(Figure 5H). The remaining organs did not show any apparent macroscopic lesions.

Histopathology Examination

Histopathological analysis showed that massive pathological damages are observed in liver, kidney, and small intestine tissues of chicken embryos in the infected group (Figure 6). Hepatic lesions included vacuolation and degeneration of hepatocytes, small numbers of hepatic

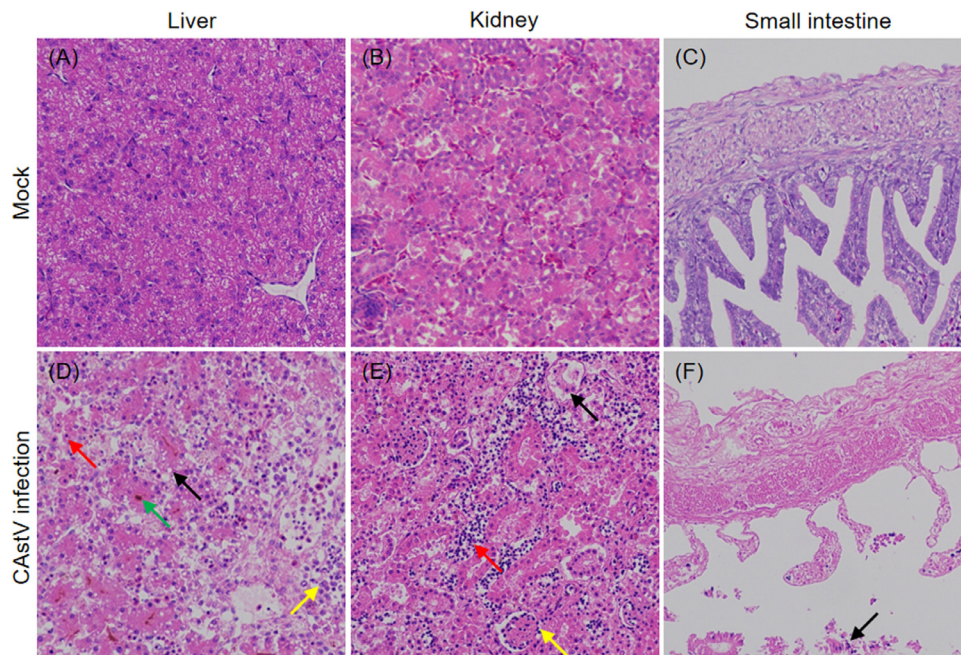


Figure 6. Histological analysis of tissue samples from 18-day-old chicken embryos infected with CAstV GD202013. (A–C) Microscopic picture of a control chicken embryo. (D–F) Microscopic picture of a CAstV-infected chicken embryo (indicated by arrows). Magnification = 200 ×. (D) Vacuolation and degeneration of hepatocytes (black arrow), small numbers of hepatic necrosis (red arrow), a few lymphocyte infiltrations around veins (yellow arrow), and accumulation of tan pigment in lobules (green arrow). (E) Massive degeneration of the epithelium in renal tubules (black arrow), dilated tubules filled with red blood cells (red arrow), unclear glomerular capillary plexus and decreased cells (yellow arrow) in the kidney. (F) Structural disorders and necrosis of epithelial cells (black arrow) in the small intestine. Abbreviation: CAstV, chicken astrovirus.

necrosis, a few lymphocyte infiltrations around veins, and accumulation of tan pigment in lobules (Figure 6D). In the kidney, massive degeneration of the epithelium in renal tubules, dilated tubules filled with red blood cells, unclear glomerular capillary plexus and decreased cells were observed (Figure 6E). Structural disorders and necrosis of epithelial cells were discovered in the small intestine (Figure 6F).

DISCUSSION

Astrovirus (**AstV**) was first described from human infants with diarrhea in 1975 (Madeley and Cosgrove, 1975), and subsequently identified in a wide range of mammalian and avian species (Snodgrass and Gray, 1977; Blomstrom et al., 2010; Donato and Vijaykrishna, 2017; Smyth, 2017). In recent years, outbreaks of chicken astrovirus have been frequently reported worldwide, and transmission of some strains can be horizontal and vertical, resulting in great economic losses to the poultry industry. Since 2016, CAstV infections showed an increasing trend in China (Xue et al., 2017; Xue et al., 2020; Zhao et al., 2020). In the current study, a novel CAstV strain GD202013 was isolated from a 1-day-old chicken flock with growth problem in Guangdong province. The novel strain affected embryonic development, reduced hatchability, and caused liver, kidney and small intestine lesions in the chicken embryos. This CAstV strain can be further used for virological and serological assay development, as well as treatment measures.

Currently, several systems are suitable for CAstV infection, such as embryonated eggs or cell culture. For example, some CAstV strains have been successfully propagated in embryonated chicken eggs, chicken embryo liver (**CEL**) cells, and chicken embryo kidney cells (**CEK**) (Bulbule et al., 2013; Palomino-Tapia et al., 2020). In addition, Zhao et al. (2020) and Kang et al. (2018) reported that the LMH is susceptible to CAstV infection. In this study, LMH cells were used to propagate CAstV GD202013 to a high titer ($10^{6.33}$ TCID₅₀/mL at passage five).

CAstV infections have been detected circulating in China, and reported by Xue et al. (2017). The full genome of four Chinese CAstV strains (CZ1701/CN/2017, HBLP717-1/CN/2018, NJ1701/CN/2017 and GDYHTJ718-6/CN/2018) described by Xue et al. (2020) and Zhao et al. (2020), were classified as subgroup Bi. In this study, the complete genome of GD202013 strain was 7,520 nucleotides in length. The results of the phylogenetic analysis showed that the new isolate GD202013 has the highest identity with 2 US CAstV strains belonging to the subgroup Bii, based on the whole genome and capsid protein. However, phylogenetic trees of the ORF1a and ORF1b did not follow the cluster pattern observed on the whole genome and capsid protein (ORF2) phylogenetic trees, which is suggestive of a recombination event. The recombinant analysis including RDP, SimPlot, and phylogenetic analysis further showed that

GD202013 is a recombinant strain formed by 3 strains: a major parent strain CkP5/US/2016 (subgroup Biv), and 2 minor parent strain GA2011/US/2011 (subgroup Bii) and G059/PL/2014 (subgroup Aiii). Genetic recombination plays an important role in the evolution of RNA viruses, which may produce new viruses with potentially different virulence and pathogenesis (Worobey and Holmes, 1999). In addition, astrovirus recombination events have been reported in poultry, for example, guinea fowl (De Battisti et al., 2012), ducks (Liu et al., 2014), turkeys (Pantin-Jackwood et al., 2006; Strain et al., 2008), and chickens (Palomino-Tapia et al., 2020). Multiple recombination regions have been detected for some CAstV isolates, including ORF1a, ORF1b, and ORF2 genes (Palomino-Tapia et al., 2020). These recombination events emphasize the importance of conducting phylogenetic analysis from the full genome sequence, rather than a single gene. These results also imply that the analyses of recombination among the CAstV strains should routinely be performed for detection of the novel CAstV recombinants.

The capsid protein is responsible for the variation in antigenicity and pathogenicity. For example, some studies showed that “white chicks” hatchery disease is associated with CAstV subgroup Bii, subgroup Biv, and subgroup Aiii (Smyth et al., 2013; Long et al., 2018; Palomino-Tapia et al., 2020), and visceral gout is related to CAstV subgroup Biii (Bulbule et al., 2013), as well as hatchability reduction is associated with CAstV subgroup Bi (Zhao et al., 2020). In this study, the infection experiment with CAstV GD202013 strain was studied in SPF chicken embryos. It showed that the strain causes hatchability reduction, growth depression and death of embryos. Macroscopic and microscopic lesions in the liver, kidney and small intestine were observed in the dead-in-shell embryos, which is similar to observations in other CAstV infections (Nunez et al., 2015; Sajewicz-Krukowska et al., 2016; Long et al., 2018). In addition, the kidney contained higher levels of viral load compared with the other tissues, indicating that the GD202013 strain replicates very well in the kidney, which is in agreement with some reports described previously (Sajewicz-Krukowska et al., 2016; Long et al., 2018).

In summary, we isolated a field strain of CAstV from a chicken flock with growth problem. Phylogenetic analysis, based on the whole genome and capsid protein, showed that the new isolate manifests a close relationship with GA2011/US/2011 belonging to the subgroup Bii. Recombination analysis indicated that the CAstV GD202013 is a recombinant strain formed by 3 strains: a major parent strain CkP5/US/2016 and 2 minor parent strains GA2011/US/2011 and G059/PL/2014. In addition, hatchability reduction, growth depression, and death of embryos were observed in the chicken embryo infection experiment. To our knowledge, this is the first study reporting the isolation and molecular characterization of a recombinant strain of CAstV, which belongs to the

subgroup Bii in China. Our results could enrich the body of information on the molecular epidemiology and pathogenicity of CAstV.

ACKNOWLEDGMENTS

This study was supported by the Science and Technology Program of Wen's Foodstuffs Group Co, Ltd (WENS2020-3), and Guangdong Basic and Applied Basic Research Foundation (2019B1515210008).

DISCLOSURES

The authors declare no conflict of interest.

SUPPLEMENTARY MATERIALS

Supplementary material associated with this article can be found, in the online version, at doi:10.1016/j.psj.2021.101363.

REFERENCES

- Baxendale, W., and T. Mebatsion. 2004. The isolation and characterization of astroviruses from chickens. *Avian Pathol.* 33:364–370.
- Blomstrom, A. L., F. Widen, A. S. Hammer, S. Belak, and M. Berg. 2010. Detection of a novel astrovirus in brain tissue of mink suffering from shaking mink syndrome by use of viral metagenomics. *J. Clin. Microbiol.* 48:4392–4396.
- Bulbule, N. R., K. D. Mandakhalikar, S. S. Kapgate, V. V. Deshmukh, K. A. Schat, and M. M. Chawak. 2013. Role of chicken astrovirus as a causative agent of gout in commercial broilers in India. *Avian Pathol.* 42:464–473.
- De Battisti, C., A. Salviato, C. M. Jonassen, A. Toffan, I. Capua, and G. Cattoli. 2012. Genetic characterization of astroviruses detected in guinea fowl (*Numida meleagris*) reveals a distinct genotype and suggests cross-species transmission between turkey and guinea fowl. *Arch. Virol.* 157:1329–1337.
- Donato, C., and D. Vijaykrishna. 2017. The broad host range and genetic diversity of mammalian and avian astroviruses. *Viruses* 9:1–18.
- Kang, K. L., E. Linnemann, A. H. Icard, V. Durairaj, E. Mundt, and H. S. Sellers. 2018. Chicken astrovirus as an aetiological agent of runt-ing-stunting syndrome in broiler chickens. *J. Gen. Virol.* 99:512–524.
- Kouwenhoven, B., M. Vertommen, and J. H. H. van Eck. 1978. Runt-ing and leg weakness in broilers: involvement of infectious factors. *Vet. Sci. Commun.* 2:253–259.
- Li, J., H. Wang, L. Mao, H. Yu, X. Yu, Z. Sun, X. Qian, S. Cheng, S. Chen, J. Chen, J. Pan, J. Shi, and X. Wang. 2020. Rapid genomic characterization of SARS-CoV-2 viruses from clinical specimens using nanopore sequencing. *Sci. Rep.* 10:17492.
- Liu, N., F. Wang, J. Shi, L. Zheng, X. Wang, and D. Zhang. 2014. Molecular characterization of a duck hepatitis virus 3-like astrovirus. *Vet. Microbiol.* 170:39–47.
- Li, Y. P., K. J. Handberg, S. Kabell, M. Kusk, M. F. Zhang, and P. H. Jorgensen. 2007. Relative quantification and detection of different types of infectious bursal disease virus in bursa of Fabricius and cloacal swabs using real time RT-PCR SYBR green technology. *Res. Vet. Sci.* 82:126–133.
- Li, Z., Y. Wang, X. Li, X. Li, H. Cao, and S. J. Zheng. 2013. Critical roles of glucocorticoid-induced leucine zipper in infectious bursal disease virus (IBDV)-induced suppression of type I Interferon expression and enhancement of IBDV growth in host cells via interaction with VP4. *J. Virol.* 87:1221–1231.
- Lole, K. S., R. C. Bollinger, R. S. Paranjape, D. Gadkari, S. S. Kulkarni, N. G. Novak, R. Ingersoll, H. W. Sheppard, and S. C. Ray. 1999. Full-length human immunodeficiency virus type 1 genomes from subtype C-infected seroconverters in India, with evidence of intersubtype recombination. *J. Virol.* 73:152–160.
- Long, K. E., R. M. Ouckama, A. Weisz, M. L. Brash, and D. Ojic. 2018. White chick syndrome associated with chicken astrovirus in Ontario. *Can. Avian Dis.* 62:247–258.
- Madeley, C. R., and B. P. Cosgrove. 1975. Letter: viruses in infantile gastroenteritis. *Lancet* 2:124.
- Martin, D. P., B. Murrell, M. Golden, A. Khoosal, and B. Muhire. 2015. RDP4: detection and analysis of recombination patterns in virus genomes. *Virus Evol.* 1:v3.
- Nunez, L. F., P. S. Santander, C. Carranza, C. S. Astolfi-Ferreira, M. R. Buim, and F. A. Piantino. 2016. Detection and molecular characterization of chicken astrovirus associated with chicks that have an unusual condition known as "white chicks" in Brazil. *Poult. Sci.* 95:1262–1270.
- Nunez, L. F., S. H. Parra, E. Mettifogo, M. H. Catroxo, C. S. Astolfi-Ferreira, and F. A. Piantino. 2015. Isolation of chicken astrovirus from specific pathogen-free chicken embryonated eggs. *Poult. Sci.* 94:947–954.
- Olsen, D. E. 1977. Isolation of a reovirus-like agent from broiler chicks with diarrhea and stunting. *Proc. West. Poult. Dis. Conf.* 26:131–139.
- Palomino-Tapia, V., D. Mitevski, T. Inglis, F. van der Meer, E. Martin, M. Brash, C. Provost, C. A. Gagnon, and M. F. Abdul-Careem. 2020. Chicken astrovirus (CAstV) molecular studies reveal evidence of multiple past recombination events in sequences originated from clinical samples of White Chick Syndrome (WCS) in Western Canada. *Viruses* 12:1–20.
- Pantin-Jackwood, M. J., E. Spackman, and P. R. Woolcock. 2006. Molecular characterization and typing of chicken and turkey astroviruses circulating in the United States: implications for diagnostics. *Avian Dis.* 50:397–404.
- Pantin-Jackwood, M. J., J. M. Day, M. W. Jackwood, and E. Spackman. 2008. Enteric viruses detected by molecular methods in commercial chicken and turkey flocks in the United States between 2005 and 2006. *Avian Dis.* 52:235–244.
- Sajewicz-Krukowska, J., K. Pac, A. Lisowska, A. Pikula, Z. Minta, B. Krolczewska, and K. Domanska-Blicharz. 2016. Astrovirus-induced "white chicks" condition - field observation, virus detection and preliminary characterization. *Avian Pathol.* 45:2–12.
- Sajewicz-Krukowska, J., and K. Domanska-Blicharz. 2016. Nearly full-length genome sequence of a novel astrovirus isolated from chickens with 'white chicks' condition. *Arch. Virol.* 161:2581–2587.
- Smyth, V. J. 2017. A review of the strain diversity and pathogenesis of chicken astrovirus. *Viruses* 9:1–10.
- Smyth, V. J., D. Todd, J. Trudgett, A. Lee, and M. D. Welsh. 2012. Capsid protein sequence diversity of chicken astrovirus. *Avian Pathol.* 41:151–159.
- Smyth, V. J., H. L. Jewhurst, B. M. Adair, and D. Todd. 2009. Detection of chicken astrovirus by reverse transcriptase-polymerase chain reaction. *Avian Pathol.* 38:293–299.
- Smyth, V. J., H. L. Jewhurst, D. S. Wilkinson, B. M. Adair, A. W. Gordon, and D. Todd. 2010. Development and evaluation of real-time TaqMan(R) RT-PCR assays for the detection of avian nephritis virus and chicken astrovirus in chickens. *Avian Pathol.* 39:467–474.
- Smyth, V., J. Trudgett, M. Wylie, H. Jewhurst, B. Conway, M. Welsh, E. Kaukonen, and P. Perko-Makela. 2013. Chicken astrovirus detected in hatchability problems associated with 'white chicks'. *Vet. Rec.* 173:403–404.
- Snodgrass, D. R., and E. W. Gray. 1977. Detection and transmission of 30 nm virus particles (astroviruses) in faeces of lambs with diarrhoea. *Arch. Virol.* 55:287–291.
- Strain, E., L. A. Kelley, S. Schultz-Cherry, S. V. Muse, and M. D. Koci. 2008. Genomic analysis of closely related astroviruses. *J. Virol.* 82:5099–5103.
- Walker, P. J., S. G. Siddell, E. J. Lefkowitz, A. R. Mushegian, D. M. Dempsey, B. E. Dutilh, B. Harrach, R. L. Harrison, R. C. Hendrickson, S. Junglen, N. J. Knowles, A. M. Kropinski, M. Krupovic, J. H. Kuhn, M. Nibert, L. Rubino, S. Sabanadzovic, P. Simmonds, A. Varsani, F. M. Zerbini, and A. J. Davison. 2019. Changes to virus taxonomy and the International Code of Virus Classification and Nomenclature ratified by the International Committee on Taxonomy of Viruses (2019). *Arch. Virol.* 164:2417–2429.

- Worobey, M., and E. C. Holmes. 1999. Evolutionary aspects of recombination in RNA viruses. *J. Gen. Virol.* 80(Pt 10):2535–2543.
- Xue, J., T. Han, M. Xu, J. Zhao, and G. Zhang. 2017. The first serological investigation of chicken astrovirus infection in China. *Biologicals* 47:22–24.
- Xue, J., T. Han, Y. Zhao, H. Yang, and G. Zhang. 2020. Complete genome sequence and phylogenetic analysis of novel avastroviruses circulating in China from 2016 to 2018. *Virus Res.* 278:197858.
- Zhao, W., Z. Wu, Y. Yao, A. Qin, and K. Qian. 2020. The isolation and molecular characterization of an astrovirus from "Yellow" chickens, China. *Front. Vet. Sci.* 7:581862.